Steel and Composite Structures, *Vol. 34, No. 5 (2020) 769-782*
DOI: https://doi.org/10.12989/scs.2020.34.5.769

Stability analysis of prestressed stayed steel columns with split-up crossarm systems

Pengcheng Li[1], Zhiqiang Li[1], Bin Jia[2] and Hao Wang*[3]

[1]*School of Civil Engineering, Chongqing University, Chongqing 400045, China*
[2]*Sichuan Institute of Building Research, Chengdu 610081, China*
[3]*School of Civil Engineering, Shandong Jianzhu University, Jinan 250101, China*

(*Received July 29, 2019, Revised October 16, 2019, Accepted October 21, 2019*)

Abstract. A Prestressed stayed steel column is an efficient and lightweight way with regard to enhancing the stability behaviour of a compression column. In the past, researchers primarily concentrated on investigating the behaviour of stayed steel columns with horizontal crossarms. However, this article focuses on prestressed stayed steel columns with split-up crossarm system, in which the crossarms are aslant and rotational symmetrically arranged. A mathematical formula calculating the optimal pretension that corresponds to the maximum critical buckling load was established according to geometric analysis based on the small deformation assumption. It was demonstrated that critical buckling mode of this stayed column is different from the one with horizontal crossarms. The governing imperfection direction that should be adopted in the nonlinear buckling analysis was determined in this work. In addition, the effects of crossarm inclination, stay diameter, and crossarm length on the stability behaviour were investigated. An influencing factor denotes the ratio of the load carrying capacity of the prestressed stayed steel column to the Euler load of the main column was also obtained.

Keywords: stayed column; split-up crossarm; numerical analysis; buckling load; geometric analysis

1. Introduction

Compared to traditional steel structures, prestressed steel structures are more efficient on saving the structural materials and decreasing the self-weight. It is possible for designers to design large span and slender structures using prestressed steel structure technology. And there has been several prestressed steel structural systems, such as beam string structures (Masao *et al.* 1985), prestressed stayed steel columns (PSSCs) (Li *et al.* 2016), suspend-dome (Kawaguchi *et al.* 1999), and cable-stiffened latticed shells (Li and Wu 2017). For the aforementioned prestressed steel structural systems, a PSSC is one of the simplest and typical structural system which has been used worldwide (Li *et al.* 2018). A typical PSSC comprises a main column, pretensioned stays, and crossarm systems. The crossarm systems and pretensioned stays can be flexibly set in PSSCs, and two types of commonly adopted PSSCs are shown in Fig. 1 (Yu *et al*. 2017, Liang 2019).

In the past, a large number of research work on PSSCs with four and three crossarm systems (see Fig. 1) has been intensively conducted. Hafez demonstrated the relationship between the pretension in stays and buckling load, and the mathematical formula to describe this relationship has also been derived (Hafez *et al.* 1979). Following the method of Hafez *et al.* (1979), Wadee and Li *et al.* (2017, 2018) derived the optimal pretension in stays of several different types of PSSCs, and a series numerical analyses have also been conducted to investigate the post buckling behaviour (Zschernack *et al.* 2016, Saito and Wadee 2009, Machacek *et al.* 2018). According to the previous numerical studies (Li *et al.* 2018, Saito and Wadee 2009), it has been demonstrated that the stability behaviour of PSSCs can be considerably affected by the crossarm length. Thus, a large number of analysis on the optimal configuration were conducted, and it has been found that the optimal crossarm length is corresponding to the transition point between different buckling modes (Chan *et al.* 2002, Steirteghem *et al.* 2005, Saito and Wadee 2010, Wang *et al.* 2019). Apart from the tradition application of directly bearing compression load, PSSCs have also been used in buckling restrained brace by Zhou *et al.* (2019). To validate the numerical accuracy and investigate the stability behaviours, experimental studies focus on the load carrying capacities or interactive buckling behaviour have also been conducted (De Araujo *et al.* 2008, Serra *et al.* 2015, Osofero *et al.* 2012, Martins *et al.* 2016).

However, most of the crossarms are horizontal placed in above literatures. As far as the authors are aware, only Steirteghem *et al.* (2005) conducted research on the stability behaviour of PSSCs with split-up crossarms, and the design procedure for this type of PSSCs is proposed.

*Corresponding author, Ph.D.
E-mail: wanghao19@sdjzu.edu.cn

http://www.techno-press.org/?journal=scs&subpage=6
ISSN: 1229-9367 (Print), 1598-6233 (Online)

(a) Four crossarm system

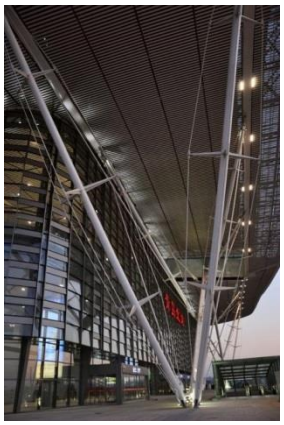

(b) Three crossarm system

Fig. 1 Structure composition of prestressed stayed steel columns

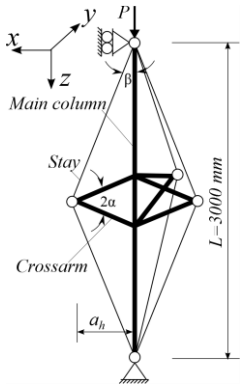

Fig. 2 Analytical model of PSSC

Table 1 Selected stay diameters and crossarm lengths

Stay diameter (mm)	1.6	3.2	4.8	6.4	8.0
Crossarm length (mm)	150	225	300	375	450

Compared to the horizontal crossarm system, the split-up crossarms could offer more lateral restraints to the main column which will potentially enhance the stability behaviour further. Thus, this article also investigate the stability behaviour of PSSCs with split-up crossarm system, but the focus is placed on the three crossarm system case (see Fig. 1(a)). As for the research method, both theoretical derivation and numerical simulation were performed in this current work. The mathematical formula to determine the optimal pretension corresponds to the maximum critical buckling load was derived by geometric analysis based on the small deformation assumption. By adopting the optimal pretension to be the benchmark, numerical analysis has also been conducted. It has been demonstrated that the geometrical distribution directions those should be adopted in the nonlinear analysis are correlated to their buckling shapes, and the parameters affecting the load carrying capacities of PSSCs have also been investigated. The influencing factor describing the relationship between the load carrying capacity and Euler load has also been presented in this work.

2. Analytical model description

2.1 Geometrical configuration

As mentioned before, the focus of this study is investigating the stability behaviour of PSSCs with split-up crossarms. The analytical model of the PSSC, which is equipped with a three-branch crossarm system, is shown in Fig. 2. As shown in Fig. 2, the PSSC is pin supported at two ends with a concentrated load P axially applied to the up end. The connections between the main column and crossarms are ideal rigid, and the connections between the stays and main column, the stays and crossarms are pinned. In Fig. 2, the symbols L and β denote the main column length and the angle between the stay and main column, respectively. The crossarm inclination, which is defined to be the angle between the crossarms and the horizontal plane, is denoted by α in Fig. 2. The projection of the crossarm length in horizontal plane is expressed by α_h.

Table 2 Experimental validation

Member types	Geometric dimensions (mm)			Material properties				$\frac{P_{FEA}}{P_{EXP}}$
	Length	Outer diameter	Inner diameter	Young's modulus (MPa)	Yield stress (MPa)	Ultimate stress (MPa)	Ultimate strain	
Main column	18000	139.92	126.58	207300	712.56	794.86	1.42%	1.087
Crossarm	535.50	101.71	84.49					

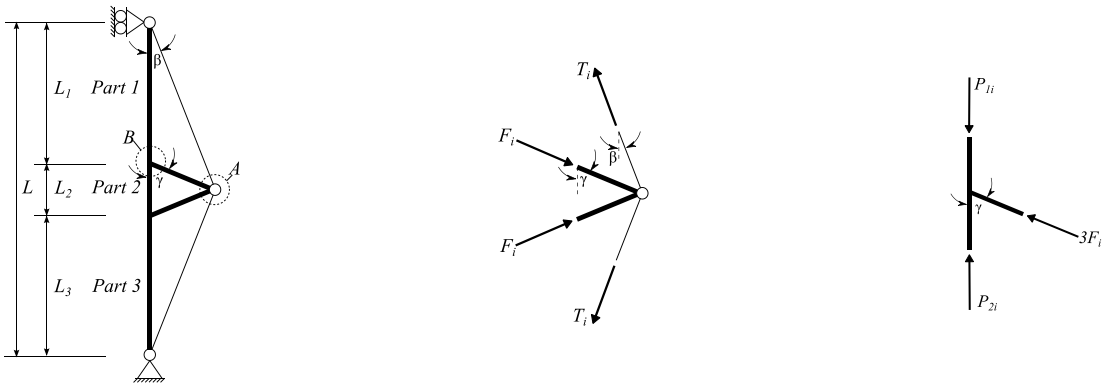

(a) 1/3 model (b) Node A (c) Node B

Fig. 3 Force analysis

To systematically investigate the behaviour of PSSCs with split-up crossarms, the stay diameter and crossarm length are varied during the numerical analysis, and the selected diameters and lengths are presented in Table 1. In addition to these two parameters, α is also an analytical parameter in this study, and the values of α is varied from 15° to 60° with an interval of 15°.

2.2 Materials and elements

The commercial software ABAQUS is adopted for the finite element analysis, shell elements (S4R) were selected to simulate the main column and crossarms, the truss elements (T2D2) were selected to simulate the stays. Owing to the stays will slack when they go to compression, thus, the truss elements were set to be "no compression" to simulate the slack phenomenon. The materials of the main column and crossarms are steel with a Young's modulus of 201000 N/mm^2, and the stay is a bar with a Young's modulus of 202000 N/mm^2 (Hafez *et al.* 1979). During the numerical analysis, all the materials are assumed to be elastic because it has been demonstrated that elastic analysis is accurate enough to estimate the stability behaviours of this type of slender stayed column.

3. Buckling analysis

3.1 Experimental validation

Both linear and nonlinear buckling analyses were performed in this study. The linear buckling analysis was conducted to determine the critical buckling loads and modes, which could be used in the nonlinear buckling analysis. Prior to conducting the numerical analysis, a comparison between the finite element and experiment results was made to ensure the accuracy of the numerical results. The experiment conducted by Martins *et al.* (2016) was selected for validation, and the comparison of FEA and experimental investigation is shown in Table 2. As it can be seen, both the main column and crossarm are fabricated from steel with circular section. According to the comparison, it can be seen that the ratio of finite element analysis result P_{FEA} to the experimental result P_{EXP} is 1.087 (see Table 2), this implies that the FEA is accurate enough to estimate the buckling load of PSSCs.

3.2 Pretension

For PSSCs, the pretension level is important for the buckling behaviour. Thus, determining the pretension in stays is important for the analysis. This study adopts the pretension corresponds to the maximum critical buckling load to be the benchmark in the numerical analysis, and this section aims to derive this pretension level.

Fig. 3(a) shows the 1/3 model of a PSSC, which comprises of the main column, one branch crossarms, and corresponding stays. For simplification, the main column can be thought to be three parts, named by Part 1, Part 2, and Part 3 from top to bottom. The axial force in Part 1 owing to the introduction of the pretensions can be calculated by Eq. (1)

$$P_{1i} = 3T_i \cos\beta \tag{1}$$

Where P_{1i} is the initial axial force in Part 1, T_i is the intial pretension in stays, and β is the angle between the stay and main column.

After applying the external load P, the axial force in Part 1 can be calculated by Eq. (2)

$$P_{1f} = P + 3T_f \cos\beta \tag{2}$$

Where P_{1f} is the final axial force in Part 1, P is the external load, T_f is the final pretension in stays.

Thus, the change of axial force in Part 1 can be expressed by Eq. (3)

$$\Delta P_1 = P + 3\cos\beta(T_f - T_i) \tag{3}$$

Taking node A to be a free body and considering the equilibrium condition in the horizontal direction (see Fig. 3(b)), the formula to calculate the axial force in crossarm owing to the introduction of pretension can be expressed by Eq. (4)

$$F_i = T_i \frac{\sin\beta}{\sin\gamma} \tag{4}$$

Where β is the angle between stay and main column, r is the angle between the crossarm and main column.

Similarly, the axial force in crossarm changed to be F_f after applying the external load P, and the expression of F_f is shown in Eq. (5)

$$F_f = T_f \frac{\sin\beta}{\sin\gamma} \tag{5}$$

Taking node B to be a free body and considering the equilibrium condition in the vertical direction (see Fig. 3(c)) and considering the relationships of Eqs. (1) and (4), the initial axial force in Part 2 owing to the introduction of the pretensions can be calculated by Eq. (6)

$$P_{2i} = 3T_i \frac{\sin\gamma\cos\beta - \sin\beta\cos\gamma}{\sin\gamma} \tag{6}$$

The final axial force in Part 2 after applying the external load P can be expressed by Eq. (7)

$$P_{2f} = P + 3T_f \frac{\sin\gamma\cos\beta - \sin\beta\cos\gamma}{\sin\gamma} \tag{7}$$

Thus, the change of axial force in Part 2 can be calculated from Eqs. (6) and (7), and can be expressed by

$$\Delta P_2 = P + 3(T_f - T_i) \cdot \frac{\sin\gamma\cos\beta - \sin\beta\cos\gamma}{\sin\gamma} \tag{8}$$

Fig. 4 depicts the configuration change of the 1/3 model after applying the external concentrated load. Based on small deformation assumption, the change of stay length Δ_s can be calculated by Eq. (9) (see Fig. 4)

$$\Delta_s = \Delta_{c1}\cos\beta - \Delta_h \sin\beta \tag{9}$$

Where Δ_h is the horizontal displacement of the crossarm end, Δ_{c1} is the vertical displacement of the upper end of the main column which can be calculated from Eq. (10).

$$\Delta_{c1} = P\left(\frac{1}{K_{c1}} + \frac{1}{2K_{c2}}\right) + 3(T_f - T_i)\left[\frac{\cos\beta}{K_{c1}} + \frac{1}{2K_{c2}} \cdot \frac{\sin\gamma\cos\beta - \sin\beta\cos\gamma}{\sin\gamma}\right] \tag{10}$$

Where K_{c1} and K_{c2} are the axial stiffness of Part 1 and Part 2.

The relationship between the change of pretension and stay length can be also expressed by Eq. (11).

$$\Delta_s = \frac{T_i - T_f}{K_s} \tag{11}$$

Similarly, the change of crossarm length after applying the external load can be calculated by Eq. (12) based on small deformation assumption.

$$\Delta_a = \Delta_{c2}\cos\gamma - \Delta_h \sin\gamma \tag{12}$$

Where Δ_h is the horizontal displacement of the crossarm end, Δ_{c2} is the vertical displacement of the intersection point of the crossarm and main column (see Fig. 4) which can be calculated by Eq. (13).

$$\Delta_{c2} = \frac{1}{2K_{c2}}\left[P + 3(T_f - T_i)\frac{\sin\gamma\cos\beta - \sin\beta\cos\gamma}{\sin\gamma}\right] \tag{13}$$

The change of crossarm length can be calculated by Eq. (14).

$$\Delta_a = \frac{F_i - F_f}{K_a} \tag{14}$$

Where K_a is the axial stiffness of the crossarm.

The horizontal displacement of the crossarm Δ_h can be calculated by Eq. (15), by combining the Eqs. (4), (5), (12), (13), and (14).

$$\Delta_h = \frac{P\cos\gamma}{2K_{c2}\sin\gamma} + (T_f - T_i)\left[\frac{3\cos\gamma(\sin\gamma\cos\beta - \sin\beta\cos\gamma)}{2K_{c2}\sin^2\gamma} + \frac{\sin\beta}{K_a\sin^2\gamma}\right] \tag{15}$$

Substituting Eqs. (10), (11), and (15) to Eq. (9), Eqs. (16) and (17) can be obtained.

$$T_i - T_f = PC_1 \tag{16}$$

$$C_1 = \frac{\cos\beta\left(\frac{1}{K_{c1}} + \frac{1}{2K_{c2}}\right) - \frac{\sin\beta\cos\gamma}{2K_{c2}\sin\gamma}}{\frac{1}{K_s} + \frac{3\cos^2\beta}{K_{c1}} - \frac{\sin^2\beta}{K_a\sin^2\gamma} + \frac{3\sin^2\gamma\cos^2\beta - 6\sin\gamma\sin\beta\cos\gamma\cos\beta + 3\sin^2\beta\cos^2\gamma}{2K_{c2}\sin^2\gamma}} \tag{17}$$

Substituting Eqs. (2) and (17) to Eq. (16), the following relationships can be obtained.

$$P = (P_{1f} - 3T_i\cos\beta)C_2 \tag{18}$$

$$C_2 = \frac{\frac{1}{K_s} + \frac{3\cos^2\beta}{K_{c1}} + \frac{3\sin^2\gamma\cos^2\beta - 6\sin\gamma\cos\gamma\sin\beta\cos\beta + 3\sin^2\beta\cos^2\gamma}{2K_{c2}\sin^2\gamma} - \frac{\sin^2\beta}{K_a\sin^2\gamma}}{\frac{1}{K_s} + \frac{3\sin^2\beta\cos^2\gamma - 3\sin\gamma\cos\gamma\sin\beta\cos\beta}{2K_{c2}\sin^2\gamma} - \frac{\sin^2\beta}{K_a\sin^2\gamma}} \tag{19}$$

From Eqs. (16) and (18), the optimal pretension corresponds to the maximum critical buckling load can be expressed by Eq. (19).

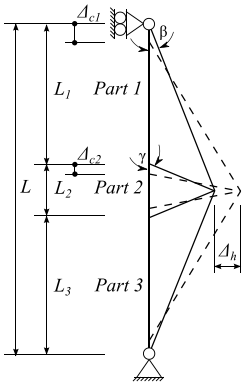

Fig. 4 Geometric deformation of 1/3 model

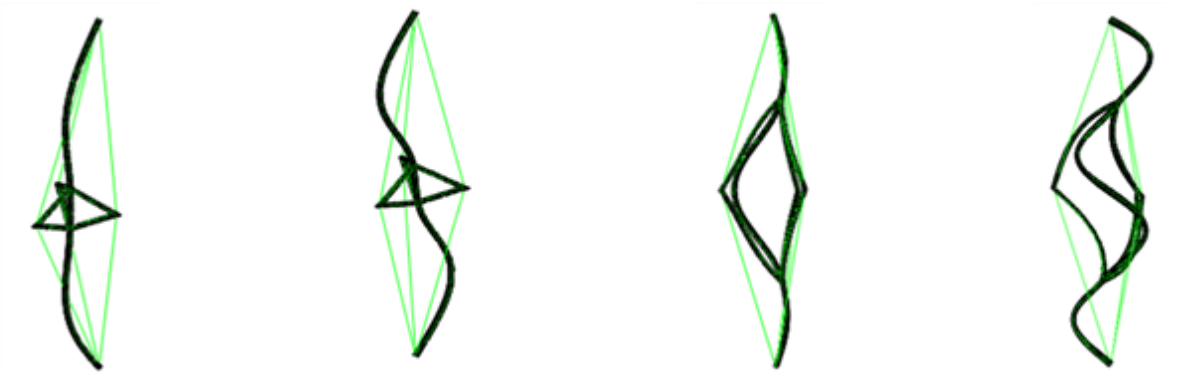

(a) Mode 1 (b) Mode 2 (c) Mode 3 (d) Mode 4

Fig. 5 Typical buckling modes

$$T_{opt} = P^{c}_{T=0} \frac{C_1}{C_2} \tag{20}$$

Where $P^{c}_{T=0}$ is the buckling load when the initial pretension is zero.

3.3 Linear buckling analysis

In this article, linear buckling analyses were conducted at first to overall investigate the stability behaviour of PSSCs. In this section, the PSSCs with all the structural parameters introduced in Section 2 were analysed. According to linear buckling analyses, it can be demonstrated that there are four different typical buckling modes for PSSCs with split-up three crossarm systems, as shown in Fig. 5. For simplification, the four typical buckling modes are named by Mode 1, Mode 2, Mode 3, and Mode 4. However, it should be noted that the critical buckling mode of this type of PSSCs can be only symmetric modes, which is Mode 1 (see Fig. 5(a)) or Mode 3 (see Fig. 5(c)). This results is different with that of a PSSC with horizontal crossarm system whose critical buckling mode can be symmetric or anti-symmetric (Saito and Wadee 2009), because there are two lateral restraint points in split-up crossarm systems.

For PSSCs with horizontal crossarms, it has been demonstrated that the interactive buckling should be considered when determining their stability behaviours, because different buckling modes can be activated simultaneously. However, whether the situation is the same in PSSCs with split-up crossarms is unknown. Thus, examining whether the interactive buckling will govern the load carrying capacities also becomes the work of this section. For simplication, the following sections adopted the term “crossarm length” to represent the projection length of the crossarm in the horizontal plane. Fig. 6 presents the first two buckling loads of PSSCs with crossarm length varying when the stay diameters equal 4.8 mm and 8.0 mm. It can be found that the critical buckling loads are always lower than the second order buckling loads, in other words, the interactive buckling can be ignored in the buckling analysis. It should be pointed out that the increase of crossarm length and inclination means a large distance between the two lateral restraint points of the crossarm systems. Because of this, the middle part of the main column, which corresponds to the part between the two lateral restraint points, could buckling at first at extremely case. Thus, the critical buckling load of $a_h = 450\ mm$ is lower than that of $a_h = 375\ mm$ when the crossarm inclination is 60° (see Fig. 6(b)).

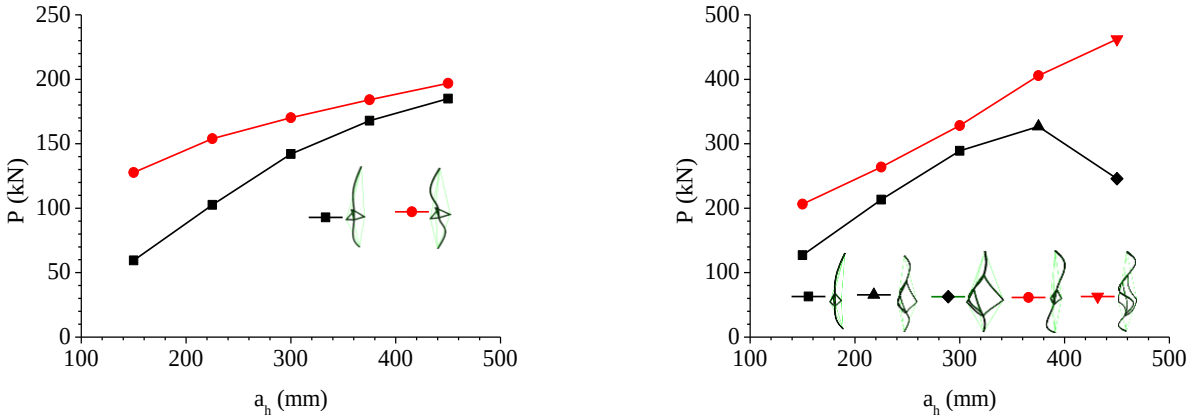

(a) ϕ=4.8 mm, α = 30° (b) ϕ=8.0 mm, α = 60°

Fig. 6 Buckling loads with different parameters

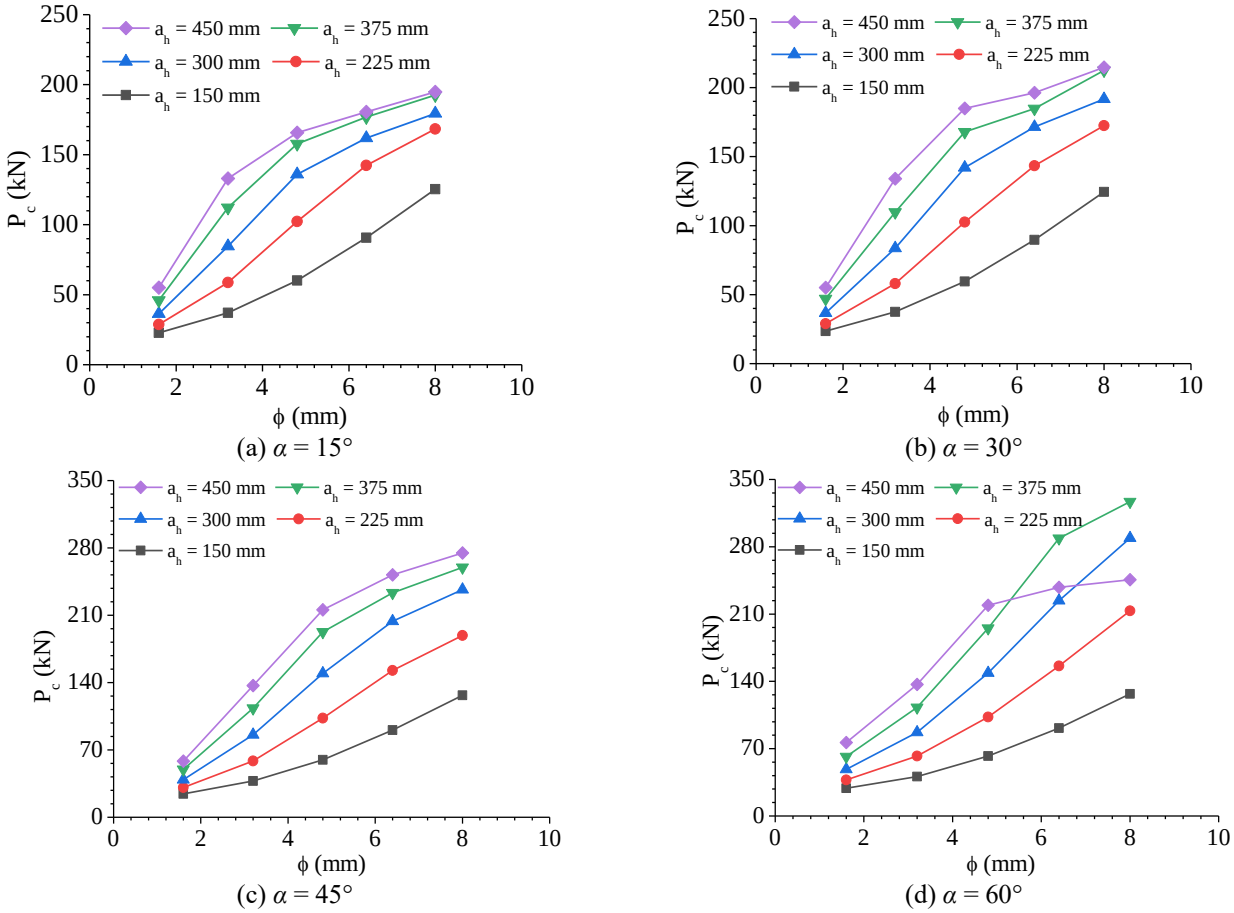

(a) α = 15° (b) α = 30°

(c) α = 45° (d) α = 60°

Fig. 7 Critical buckling loads with different parameters

Fig. 7 presents the critical buckling loads with stay diameter and crossarm length varying. Obviously, the critical buckling load can be generally enhanced by the stay diameter and crossarm length. In Fig. 7(d), it should be noted that the curve for $a_h = 450\ mm$ intersects with another two curves of $a_h = 300\ mm$ and $a_h = 375\ mm$ when the stay diameter is greater than 4.8 mm, this is also because of the buckling mode variety owing to the stiffness changes. For PSSCs, the increase of stay diameter results in the increase of lateral restraint stiffness afford by the crossarms. Thus, the buckling mode changes from Mode 1 to Mode 3 with a slowly increase of buckling load for the case of $a_h = 450\ mm$ when the stay diameter is no more than 4.8 mm.

Table 3 Geometric imperfections

Direction / Shape	x		y	
	Positive	Negative	Positive	Negative
Mode 1	1-x-P	1-x-N	1-y-P	1-y-N
Mode 3	3-x-P	3-x-N	3-y-P	3-y-N

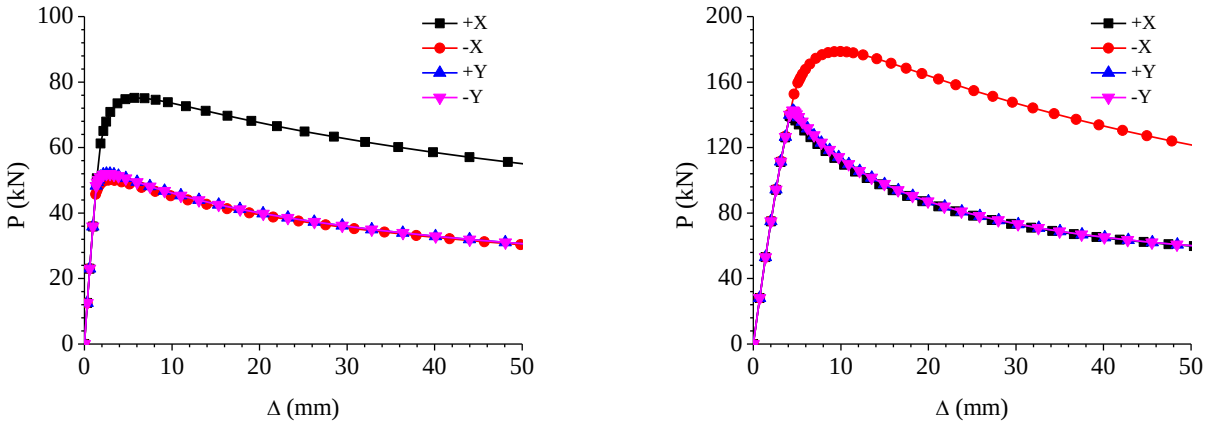

(a) ϕ=4.8 mm, a_h =300 mm, α = 30° (b) ϕ=8 mm, a_h =375 mm, α = 60°

Fig. 8 Load versus end-shortening curves with geometric imperfections in different directions

In contrast, the buckling mode cannot be changed by the stay diameter increase when $a_h = 300\ mm$ and $a_h = 375\ mm$. For these two cases, the buckling loads are always considerably improved by increasing the stay diameter. Consequently, there are two intersection points in Fig. 7(d).

3.4 Nonlinear buckling analysis

3.4.1 Governing imperfection directions

As shown in Fig. 6, the buckling loads do not intersect with each other, this implies that the buckling modes with different shapes cannot be triggered simultaneously. In other words, it is not necessary to consider the interactive buckling in PSSCs with split-up three crossarm system. Thus, this current work adopt the critical buckling mode shape to determine the geometric imperfection shape. However, it must be pointed out that the critical buckling modes shown in Figs. 5(a) and 5(c) could occur in the x and y directions. Thus, the geometric imperfection directions should be carefully examined because the crossarms are asymmetric set around the main column (see Fig. 2). Owing to this crossarm arrangment scheme, the stability behaviour of the stayed column may be different when same geometric imperfection shapes are introduced in different directions. The aim of this section is to determine the governing imperfection directions in nonlinear buckling analysis. Note that the critical buckling modes can be only Mode 1 and Mode 3 as demonstrated in the first paragraph of Section 3.3, thus, there are 8 different cases those should be considered in this section as summarised in Table 3. In Table 3, the numbers "1" and "3" are adopted to represent the imperfection shapes are the same with Mode 1 and Mode 3. The symbols "x", "y", "P", and "N" in Table 3 are adopted to denote the imperfection directions. For example, the expression "1-x-P" denote the geometric imperfection shape adopted in nonlinear buckling analysis is the same with Mode 1, and mid-span out of straightness is in the positive x directions.

Fig. 8 presents the load versus end-shortening curves with geometric imperfections in different directions. In Fig. 8(a), the corresponding critical buckling mode is Mode 1, and that of Fig. 8(b) is Mode 3. For Fig. 8(a), the governing imperfection direction is –x; for Fig. 8(b), the governing imperfection direction is +x. In addition to the two cases shown in Fig. 8, the PSSCs with all the parameters introduced in Section 2 have also been investigated though the results have not been presented in this section. It shows that the governing direction for Mode 1 is in the –x direction, but that for Mode 3 is in the +x direction for the parameters analysed in this work. This is the principle to determine the governing imperfection direction in the nonlinear buckling analysis.

3.4.2 Post buckling behaviour

To investigate the post buckling behaviour, nonlinear buckling analyses considering the initial imperfections must be performed. In the nonlinear buckling analysis, the imperfection magnitude is assumed to be L/300 (L is the main column length). In this section, eight analytical models named from "Model 1" to "Model 8" (see Table 4) were selected for the post buckling analysis. It should be noted that the cases $\alpha = 0^\circ$ denote the PSSCs with horizontal crossarm systems.

Table 4 Selected analytical models for post buckling analysis

ϕ=4.8 mm, a_h=300 *mm*				ϕ=8.0 mm, a_h=375 *mm*			
$\alpha=0^\circ$		$\alpha=30^\circ$		$\alpha=0^\circ$		$\alpha=60^\circ$	
$T=0$	$T=T_{opt}$	$T=0$	$T=T_{opt}$	$T=0$	$T=T_{opt}$	$T=0$	$T=T_{opt}$
Model 1	Model 2	Model 3	Model 4	Model 5	Model 6	Model 7	Model 8

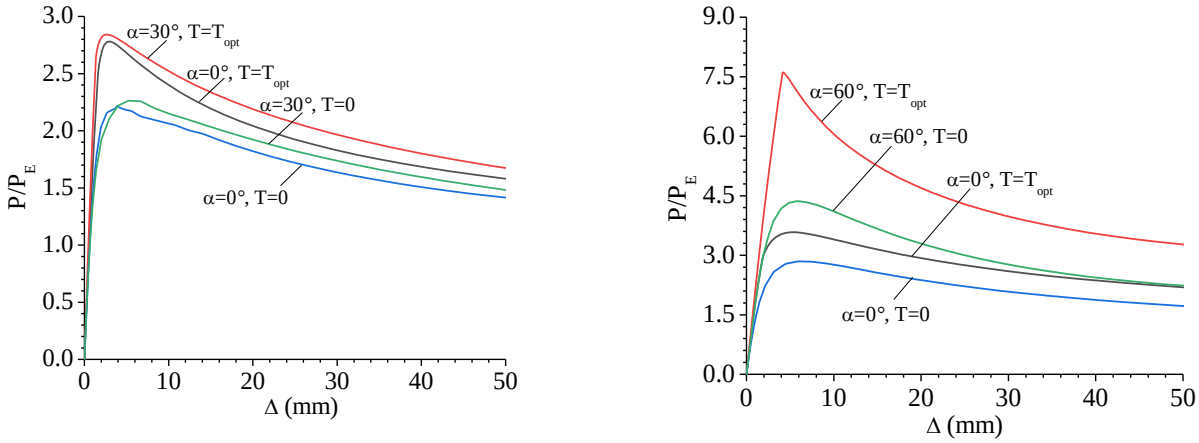

(a) ϕ=4.8 mm, a_h = 300 mm (b) ϕ=8.0 mm, a_h = 375 mm

Fig. 9 Load versus end-shortening curves

Fig. 9 presents the load versus end-shortening curves of the above eight analytical models. In Fig. 9, the vertical axes represent the ratio of axial load of PSSCs (P) to the Euler load (P_E) of corresponding main columns. It can be observed that the maximum values of P/P_E are greater than 1.0 for the models, which implies the effect of pre-tensioned stays on enhancing the stability behaviour of compression columns, because the Euler load P_E is the upper limit of compression members. From Fig. 9, it can be also seen that the split-up crossarm systems are more effective regarding to improving the stability behaviour of PSSCs than the horizontal crossarm systems. Compared the load carrying capacities of PSSCs with same crossarm layouts but different initial pretensions, it can be noted that the load carrying capacity corresponds to T_{opt} is greater than that without initial pretensions. Thus, this work adopted T_{opt} to be the benchmark for the initial pretensions in the following numerical analysis.

Fig. 10 present the buckling modes of PSSCs when the external axial load achieves the load carrying capacity. It can be seen that the post buckling mode is considerably affected by the crossarm arrangement. For the PSSCs with horizontal crossarm systems, the post buckling mode can be asymmetric (see Fig. 10(a)) when the imperfection is introduced as the critical buckling mode, because the critical buckling mode in this case could be anti-symmetric. However, the post buckling mode for PSSCs with split-up crossarm system is always symmetric when the imperfection in nonlinear analysis is introduced as the critical buckling mode, because the critical buckling mode for the structural parameters analysed in this work is always symmetric.

4. Parametric analysis

According to the above analyses, it has been seen that the load carrying capacities of PSSCs are much higher than those of traditional un-stiffened compression columns. However, owing to the unique layouts of the crossarms and stays in PSSCs with split-up crossarms, the effects of different structural parameters on the stability of this stayed column type is different. This section aims to resolve this issue by parametric analysis. In PSSCs, the stay diameter and crossarm length are two crucial factors affecting the stability behaviour, because these two factors determine the stiffness of the crossarm system. In addition to the stay diameter and crossarm length, the crossarm inclination is also a key factor affecting the stability behavior because it could affect the lateral restraint positions. Based on this situation, this section will consider these three factors.

(1) Effect of crossarm inclination

It has been proved in Section 3.2.2 that the split-up crossarm system is much effective to improving the stability behaviour of compression columns. However, the effects of crossarm inclination in split-up crossarm system is unclear. Fig. 11 present the load versus end-shortening curves of PSSCs with crossarm inclination varying. Generally, it can be observed that the load carrying capacity can be increased

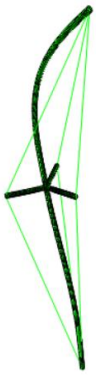

(a) ϕ=4.8 mm, $a_h = 300\ mm$, $\alpha = 0°$

(b) ϕ=4.8 mm, $a_h = 300\ mm$, $\alpha = 30°$

(c) ϕ=8.0 mm, $a_h = 375\ mm$, $\alpha = 0°$

(d) ϕ=8.0 mm, $a_h = 375\ mm$, $\alpha = 30°$

Fig. 10 Buckling modes of PSSCs when the pretension is T_{opt}.

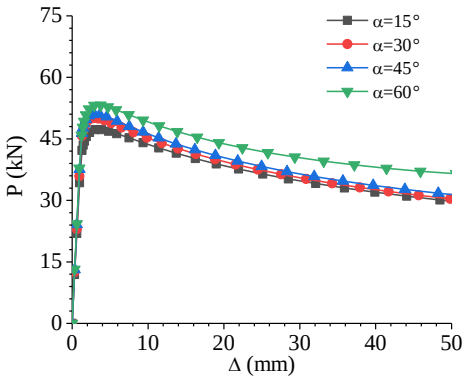

(a) ϕ=4.8 mm, a_h = 300 mm

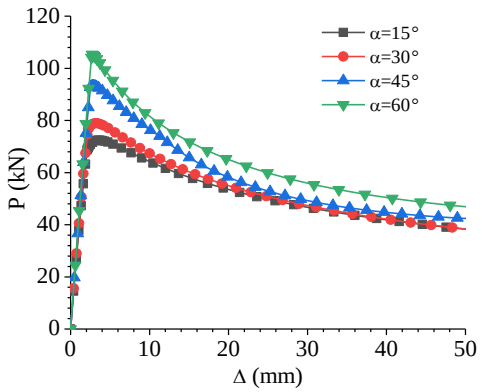

(b) ϕ=8 mm, a_h = 300 mm

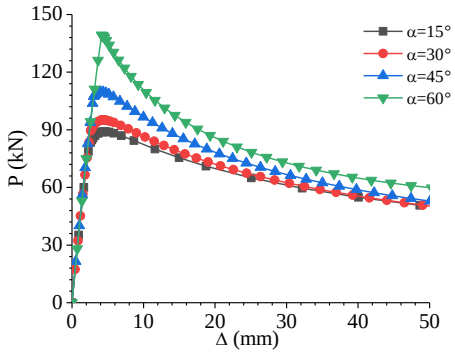

(c) ϕ=8 mm, a_h=375 mm

Fig. 11 Load versus end-shortening curves with different crossarm inclination

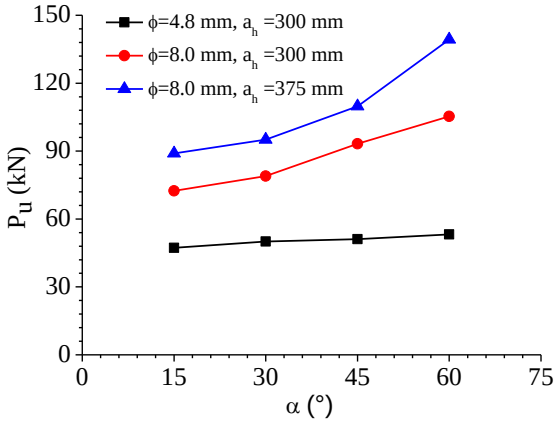

Fig. 12 Load carrying capacities with crossarm inclination varying

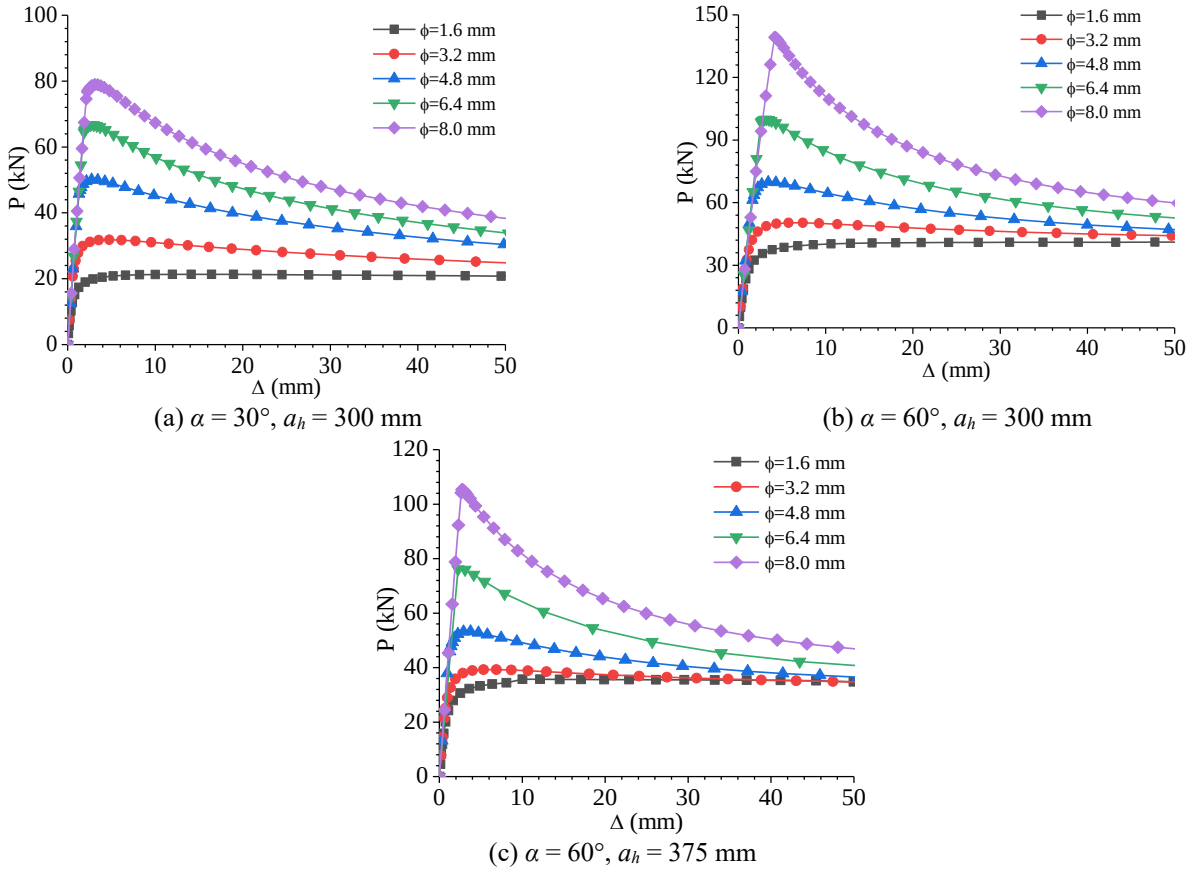

(a) $\alpha = 30°$, $a_h = 300$ mm

(b) $\alpha = 60°$, $a_h = 300$ mm

(c) $\alpha = 60°$, $a_h = 375$ mm

Fig. 13 Load versus end-shortening curves with different stay diameters

by increasing the crossarm inclination from 15° to 60°. Note that the initial slopes of the curves with different crossarm inclination are similar as shown in Fig. 11, it means that the effect of crossarm inclination on the initial structural stiffness of PSSCs can be ignored, though it affects the load carrying capacity considerably.

Fig. 12 demonstrates the load carrying capacities of PSSCs with split-up crossarm systems when the crossarm inclination varies from 15° to 60°. It can be seen from Fig. 12 that increasing the crossarm inclination is especially effective when the crossarm length is large, this is because large crossarm length with large inclination could decrease the constraint length between the column ends and crossarm ends, which could result in the capacity improvement.

(2) Effect of stay diameter

To investigate the effect of stay diameter on the behaviour of PSSCs, the stay diameter was varied from 1.6 mm to 8.0 mm with an interval of 1.6 mm in this section. Fig. 13 presents the axial load versus end-shortening curves of PSSCs with different stay diameters. Obviously,

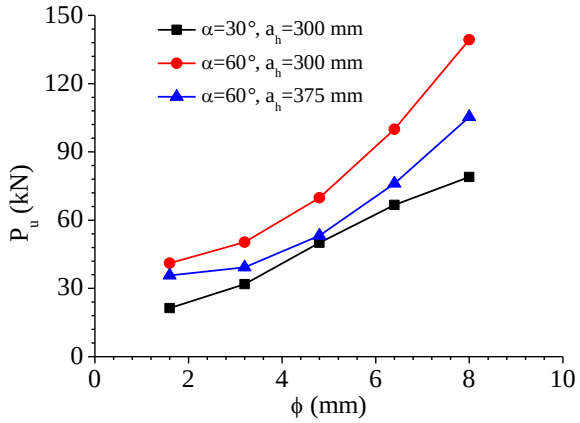

Fig. 14 Load carrying capacities with stay diameter varying

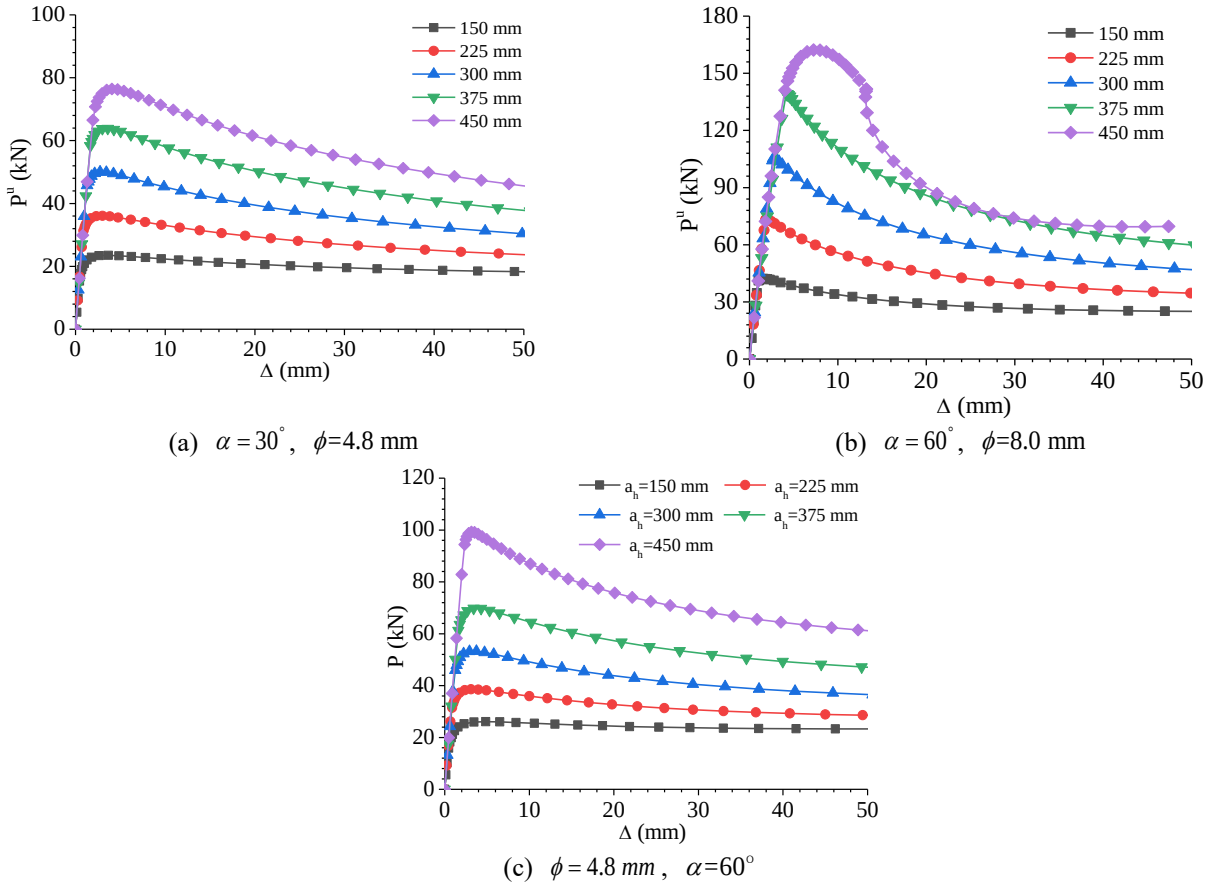

Fig. 15 Load versus end-shortening curves with different crossarm lengths

increasing the stay diameter could enhance the load carrying capacity of PSSCs. However, it should be noted that the structural stiffness after the buckling occurs could be decreased by increasing the stay diameter, though the stay diameter could not affect the initial structural stiffness.

Fig. 14 present the load carrying capacities with stay diameter varying. It can be observed that increasing the stay diameter could improve the load carrying capacities, however, this effect is also affected by the crossarm inclination and crossarm length. When the crossarm inclination or crossarm length is large, it is more effective to enhance the load carrying capacity by increasing the stay diameter.

(3) Effect of crossarm length

The crossarm length was varied from 150 mm to 450 mm with an interval of 75 mm in this section in order to study the effect of crossarm length on the stability behaviour of PSSCs with split-up crossarm systems.

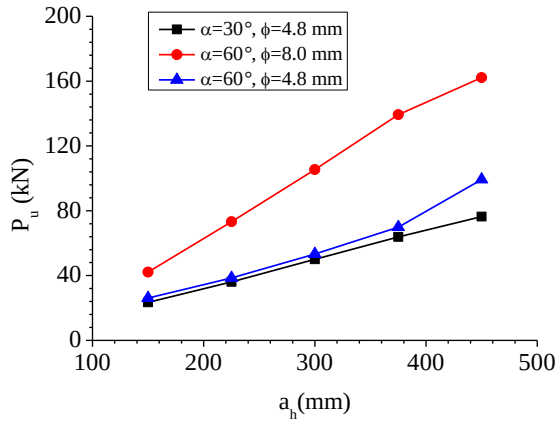

Fig. 16 Load carrying capacities with crossarm length varying

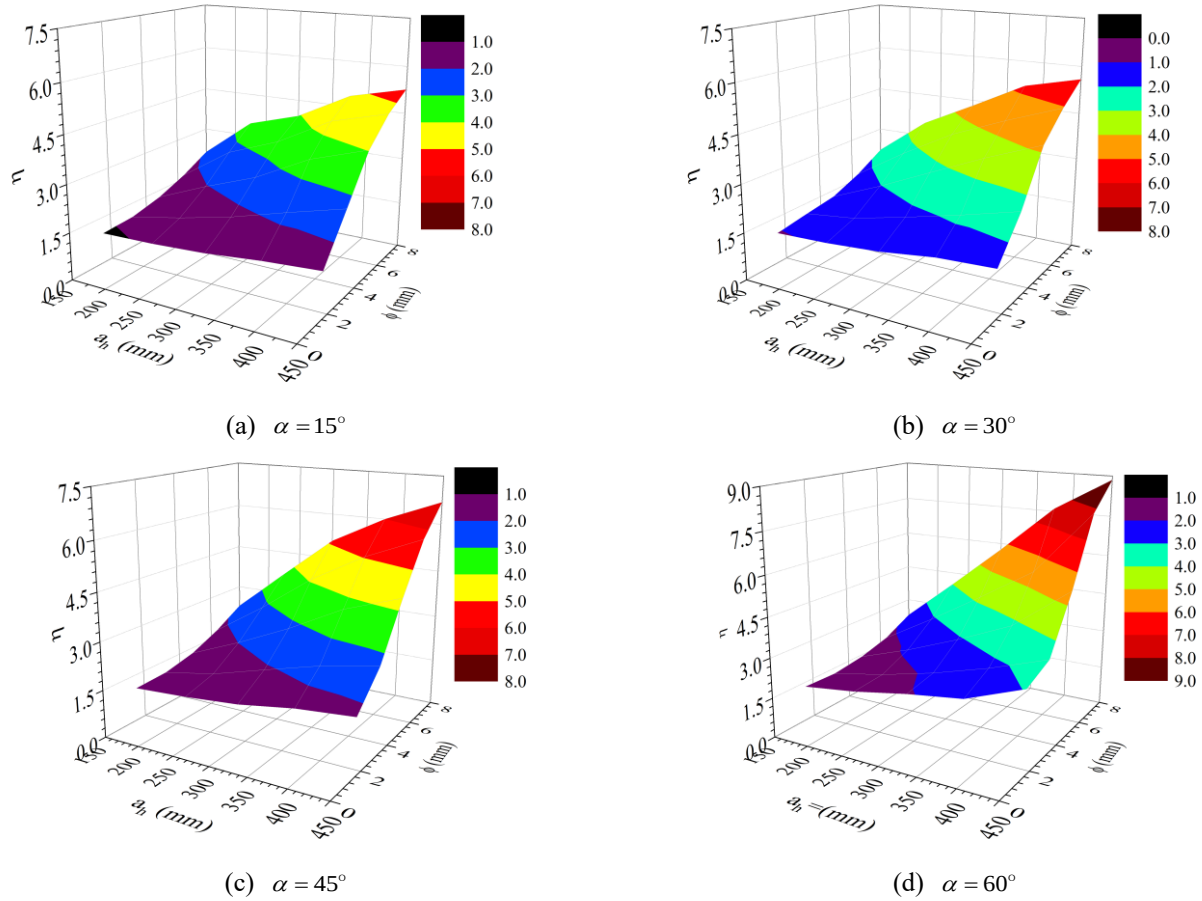

(a) $\alpha = 15^{\circ}$ (b) $\alpha = 30^{\circ}$

(c) $\alpha = 45^{\circ}$ (d) $\alpha = 60^{\circ}$

Fig. 17 Relationship between the influence coefficient and structural parameters

Fig. 15 shows the axial load versus end-shortening curves of PSSCs with crossarm length varying, and the load carrying capacities have also been presented in Fig. 16. Obviously, increasing the crossarm length within 150 mm to 450 mm can enhance the load carrying capacities. Similar to the effect of stay diameter, increasing the crossarm length could decrease the structural post-buckling stiffness, though it could not affect the initial structural stiffness.

5. Discussion

The effects of crossarm inclination, stay diameter, and crossarm length on the post buckling behaviour of PSSCs with split-up crossarms have been qualitatively investigated above. This section will quantitatively discuss the effects of the above three parameters on the load carrying capacities. To achieve this, an influence coefficient η is defined in

Eq. (21).

$$\eta = \frac{P_u}{P_E} \tag{7}$$

Where P_u is the load carrying capacity of PSSC, and P_E is the Euler's load.

Fig. 17 shows the relationships between the influence coefficients and the crossarm length and stay diameter with different crossarm inclinations. Obviously, it can be seen that the influence coefficient varies from around 1.0 to 8.0 for the structural parameters analysesed in this section. It must be noted that the case $\eta = 1.0$ does not mean it is not useful to adopt the pre-tensioned stays improving the capacities of compression columns, because the Euler's load P_E does not consider the nonlinear behaviour and imperfections of the columns; in contrast, the load carrying capacity P_u is the actual capacity which considered the nonlinear behaviour and imperfections.

Eq. (22) presents the fitted mathematical expression of η by using the least square method. Recalling the definition of η, it is also possible to estimate the load carrying capacities without performing finite element analysis by using the structural parameters and material properties.

$$\eta = \begin{cases} 1.413 - (0.8817e-2)a_h - 0.27\phi + (1.903\text{e}-5)a_h^2 + (0.3649e-2)a_h\phi - (6.222\text{e}-9)a_h^3 - (3.765\text{e}-6)a_h^2\phi & (22a) \\ 2.244 - (0.4276e-2)a_h - 1.214\phi + (0.4013e-2)a_h\phi + 0.1914\phi^2 - (0.2559e-3)a_h\phi^2 - (0.7939e-2)\phi^3 & (22b) \\ 0.3494 - (0.3559e-2)a_h - 0.289\phi - (6.842\text{e}-6)a_h^2 + (0.2065e-2)a_h\phi + (0.226e-1)\phi^2 & (22c) \\ 3.096 - (0.8634\text{e}-2)a_h - 0.9454\phi + (1.397\text{e}-5)a_h^2 + (0.2881e-2)a_h\phi + (0.7041e-1)\phi^2 & (22d) \end{cases}$$

6. Conclusions

This study addressed the stability behaviour of a PSSC with a split-up three crossarm system. This was attained through geometric derivation and finite element analysis. The following main conclusions can be obtained from this study:

- The relationship between the initial pretension and critical buckling load was geometrically investigated, and a mathematical formula to describe this relationship was derived based on small deformation assumption. The optimal initial pretension corresponding to the critical buckling load has been suggested.
- It has been shown from linear buckling analysis that the typical critical buckling mode of PSSCs with split-up crossarm system is complex, which distinguishes from that of PSSCs with horizontal crossarm systems.
- The governing imperfection shapes and directions of PSSCs with split-up three crossarm systems have been demonstrated in this study, it has been proved that the initial imperfection must be introduced in parallel with the crossarm layout directions, other than perpendicular to the crossarm layout directions.
- It has also demonstrated that the split-up crossarm system is more effective than the horizontal crossarm system regarding to enhancing the load carrying capacities. The effects of different structural parameters on the stability behaviour have been studied, and a fitting formula predicts the relationship between the load carrying capacity and Euler's load has been proposed.

Acknowledgements

The research was supported by the Fundamental Research Funds for the Central Universities (No. 2019CDXYTM0032), the National Natural Science Foundation of China (No. 51808070), and the Fundamental and Frontier Research Project of Chongqing (No. cstc2018jcyjAX0535). These financial supports are gratefully acknowledged.

References

Chan, S., Shu, G. and Lü, Z. (2002), "Stability analysis and parametric study of pre-stressed stayed columns", *Eng. Struct.*, **24**(1), 115-124. https://doi.org/10.1016/S0141-0296(01)00026-8.

De Araujo, R.R., *et al.* (2008), "Experimental and numerical assessment of stayed steel columns", *J. Constr. Steel Res.*, **64**, 1020-1029. https://doi.org/10.1016/j.jcsr.2008.01.011.

Zhou, P., *et al*. (2019), "Load resistance and hysteretic response of multiple cross-arm pre-tensioned cable stayed buckling-restrained braces", *Eng. Struct.*, **183**, 949-964. https://doi.org/10.1016/j.engstruct.2019.01.078.

Hafez, H.H., Temple, M.C. and Ellis, J.S. (1979), "Pre-tensioning of single-crossarm stayed columns", *J. Struct. Division*, **105**(2), 359-375.

Kawaguchi, M., Abe, M. and Tatemichi, I. (1999), "Design, tests and realization of 'suspen-dome' system", *J. Int. Assoc. Shell Spatial Struct.*, **40** (131), 179-192.

Lapira, L., Wadee, M.A. and Gardner, L. (2017), "Stability of multiple-crossarm prestressed stayed columns with additional stay systems", *Structures*, **12**, 227-241. https://doi.org/10.1016/j.istruc.2017.09.010.

Li, P.C., Wadee, M.A., Yu, J.L., Christie, N.G. and Wu, M.E. (2016), "Stability of prestressed stayed steel columns with a three branch crossarm system", *J. Constr. Steel Res.*, **122**, 274-291. https://doi.org/10.1016/j.jcsr.2016.03.007.

Li, P.C. and Wu, M.E. (2017), "Stabilities of cable-stiffened cylindrical single-layer latticed shells", *Steel Compos. Struct.*, **24**(5), 591-602. https://doi.org/10.12989/scs.2017.24.5.591.

Li, P.C., Liu, X. and Zhang, C.L. (2018), "Interactive buckling of cable-stiffened steel columns with pin-connected crossarms", *J. Constr. Steel Res.*, **146**, 97-108. https://doi.org/10.1016/j.jcsr.2018.03.037.

Li, P.C., Liang, C., Yuan, J. and Qiao, K. (2018), "Stability of steel columns stiffened by stays and multiple crossarms", *J. Constr. Steel Res.*, **148**, 189-197. https://doi.org/10.1016/j.jcsr.2018.05.020.

Liang, C. (2019), "Investigation into the load carrying capacities of prestressed stayed steel columns", MS. Dissertation, Southwest University, Chongqing. (in Chinese).

Masao, S. and Kurasiro, T. (1985), "A study on structural behaviors of beam string structure", *Summaries of technical papers of annual meeting architectural institute of Japan*, Tokyo, Japan, B, **1**, 280-284.

Martins, J.P., Shahbazian, A., da Silva, L.S., Rebelo, C. and Simões R. (2016), "Structural behavior of prestressed stayed

columns with single and double cross-arms using normal and high strength steel", *Arch. Civil Mech. Eng.*, **16**(4), 618-633. https://doi.org/10.1016/j.acme.2016.04.004.

Machacek, J. and Pichal, R. (2018), "Buckling and collapse capacity of prestressed steel tube stayed columns with one and two crossarms", *Thin-Wall. Struct.*, **132**, 58-68. https://doi.org/10.1016/j.tws.2018.07.045.

Osofero, A.I., Wadee, M.A. and Gardner, L. (2012), "Experimental study of critical and post-buckling behaviour of prestressed stayed column", *J. Constr. Steel Res.*, **79**, 226-241. https://doi.org/10.1016/j.jcsr.2012.07.013.

Steirteghem, J.V., *et al.* (2005), "Optimum design of stayed columns with split-up cross arm", *Adv. Eng. Softw.*, **36**(9), 614-625. https://doi.org/10.1016/j.advengsoft.2005.03.007.

Saito, D. and Wadee, M.A. (2009), "Numerical studies of interactive buckling in prestressed steel stayed columns", *Eng. Struct.*, **31**(2), 432-443. https://doi.org/10.1016/j.engstruct.2008.09.008.

Saito, D. and Wadee, M.A. (2010), "Optimal prestressing and configuration of stayed columns", *Proceedings of the Institution of Civil Engineers: Structures and Buildings*, **163**(5), 343-355.

Serra, M., *et al*. (2015), "A full scale experimental study of prestressed stayed columns", *Eng. Struct.*, **10**, 490-510. https://doi.org/10.1016/j.engstruct.2015.06.033.

Wang, H., Li, P.C. and Wu, M.E. (2019), "Crossarm length optimization and post-buckling analysis of prestressed stayed steel columns", *Thin-Wall. Struct.*, **144**, 106371. https://doi.org/10.1016/j.tws.2019.106371.

Yu, J.L. and Wadee, M.A. (2017), "Mode interaction in triple-bay prestressed stayed columns", *Int. J. Nonlinear Mech.*, **88**, 47-66. https://doi.org/10.1016/j.ijnonlinmec.2016.10.012.

Zschernack, C., Wadee, M.A. and Völlmecke, C. (2016), "Nonlinear buckling of fiber-reinforced unit cells of lattice materials", *Compos. Struct.*, **136,** 217-228. https://doi.org/10.1016/j.compstruct.2015.09.059.

DL